



Article

Carboxy-Terminal Cementum Protein 1-Derived Peptide 4 (cemp1-p4) Promotes Mineralization through wnt/ β -catenin Signaling in Human Oral Mucosa Stem Cells

Rita Arroyo¹, Sonia López¹, Enrique Romo¹, Gonzalo Montoya¹, Lía Hoz¹ , Claudia Pedraza¹, Yonathan Garfias^{2,3} and Higinio Arzate^{1,*}

¹ Laboratorio de Biología Periodontal, Facultad de Odontología, Universidad Nacional Autónoma de México, CDMX 04510, Mexico; rittaarroyo@yahoo.com.mx (R.A.); sonyletayf@hotmail.com (S.L.); dr_roaren@yahoo.com.mx (E.R.); jimago_jar@hotmail.com (G.M.); lahry@hotmail.com (L.H.); patpedrazamora@gmail.com (C.P)

² Departamento de Bioquímica, Facultad de Medicina, UNAM, Universidad Nacional Autónoma de México, CDMX 04510, Mexico; ygarfias@bq.unam.mx

³ Instituto de Oftalmología Conde de Valenciana, CDMX 06800, Mexico

* Correspondence: harzate@unam.mx

Received: 20 January 2020; Accepted: 12 February 2020; Published: 15 February 2020



Abstract: Human cementum protein 1 (CEMP1) is known to induce cementoblast and osteoblast differentiation and alkaline phosphatase (ALP) activity in human periodontal ligament-derived cells in vitro and promotes bone regeneration in vivo. CEMP1's secondary structure analysis shows that it has a random-coiled structure and is considered an Intrinsic Disordered Protein (IDP). CEMP1's short peptide sequences mimic the biological capabilities of CEMP1. However, the role and mechanisms of CEMP1's C-terminal-derived synthetic peptide (CEMP1-p4) in the canonical Wnt/ β -catenin signaling pathway are yet to be described. Here we report that CEMP1-p4 promotes proliferation and differentiation of Human Oral Mucosa Stem Cells (HOMSCs) by activating the Wnt/ β -catenin pathway. CEMP1-p4 stimulation upregulated the expression of β -catenin and glycogen synthase kinase 3 beta (GSK-3B) and activated the transcription factors TCF1/7 and Lymphoid Enhancer binding Factor 1 (LEF1) at the mRNA and protein levels. We found translocation of β -catenin to the nucleus in CEMP1-p4-treated cultures. The peptide also penetrates the cell membrane and aggregates around the cell nucleus. Analysis of CEMP1-p4 secondary structure revealed that it has a random-coiled structure. Its biological activities included the induction to nucleate hydroxyapatite crystals. In CEMP1-p4-treated HOMSCs, ALP activity and calcium deposits increased. Expression of Osterix (OSX), Runt-related transcription factor 2 (RUNX2), Integrin binding sialoprotein (IBSP) and osteocalcin (OCN) were upregulated. Altogether, these data show that CEMP1-p4 plays a direct role in the differentiation of HOMSCs to a “mineralizing-like” phenotype by activating the β -catenin signaling cascade.

Keywords: cementum; peptide; β -catenin; cell differentiation; CEMP1-p4; mineralization; stem cells

1. Introduction

The periodontium is a unique, complex and functional biological system that provides support to the dental organs. It is composed of two connective mineralized tissues—alveolar bone and cementum and two soft connective tissues, gingiva and periodontal ligament. However, the commonly occurring disease, periodontitis, leads to loss of homeostasis and consequently to the destruction of the tooth-supporting

structures [1]. Therefore, it is the aim of periodontal therapeutics to restore structurally and functionally the periodontium. For this to occur, a series of molecular events must be concerted timely and spatially. Of relevant importance for the regeneration of the periodontium is the formation of new cementum [2]. Nevertheless, the cellular and molecular mechanisms that regulate the formation of cementum are poorly understood [2]. This unique tissue covers the root surface and in conjunction with periodontal ligament and alveolar bone, provides a functional anchoring apparatus in the periodontium [3–5]. Recent evidence has shown that the lamina propria of the oral mucosa contains mesenchymal stem cell populations that can differentiate in order to form mineralized tissues [6]. A few years ago, cementum markers such as cementum protein 1 (CEMP1) and cementum attachment protein (CAP) were cloned and characterized [7,8]. These two proteins have shown to promote the proliferation and differentiation of periodontal ligament cells toward a “mineralizing-like” phenotype [9–11]. Preclinical studies have shown that CEMP1’s peptide sequences can be utilized in therapeutic interventions such as critical-sized calvarial defects, mimicking *hr*CEMP1’s (human recombinant Cementum Protein 1) biological and therapeutic capabilities [12]. Therefore, CEMP1’s short peptide sequences are possible regulators of stem cell differentiation toward a “mineralizing-like” cell phenotype [12].

The canonical Wnt/ β -catenin signalling pathway is necessary for tooth development during epithelial-mesenchymal interactions and mineralized tissue formation, indicating that β -catenin plays a critical role in this signalling pathway [13–15]. The cumulative evidence has shown how the Wnt signalling pathway coordinates pluripotency and self-renewal of stem cells [16–18]. The Wnt signaling pathway stabilizes β -catenin, which binds to the T-cell factor/lymphoid enhancer-binding factor (TCF/LEF) transcription factors and mediates the transcription of Wnt target genes [19]. However, activated Wnt/ β -catenin is not sufficient to induce osteogenic differentiation unless other stimulatory signals are present. In addition, little is known about the involvement of CEMP1’s peptide sequences on the canonical Wnt signaling pathway on cell differentiation to a “mineralizing-like” cell phenotype. Previous studies have shown that CEMP1’s N-terminal domain possesses biological properties to promote cell differentiation and mineralization. Analysis of CEMP1’s carboxy-terminus domain revealed that its secondary structure is 100% random-coiled and represents CEMP1’s most intrinsically disordered region (IDR). This polypeptide segment is likely to form a defined three-dimensional structure but is nevertheless functional. It is known that IDRs actively participate in diverse functions that increase the functional states in which a protein can exist in the cell. In this study, we aimed to determine whether CEMP1’s carboxy-terminus sequence triggers the Wnt signaling pathway in human oral mucosal stem cells (HOMSCs) to differentiate toward a “mineralizing-like” cell phenotype.

2. Results

2.1. CEMP1-p4 Physicochemical Characteristics

CEMP1-p4 has a molecular weight (MW) of 1595.72 Da with a theoretical isoelectric point of 4.03. Theoretical relative hydrophobicity is of 20.15 and GRAVY (grand average of hydrophathy) is of -1.160 . These characteristics make CEMP1-p4 a hydrophilic peptide. Circular dichroism of CEMP1-p1 showed a spectrum with negative weak signal values near to 197 nm. The spectrum reflects the random-coil CEMP1-p4 structure (Figure 1A). Dynamic light scattering analysis showed that CEMP1-p4 forms monomeric species of ~ 10 nm and polymeric aggregates of ~ 120 and ~ 5000 nm (Figure 1B).

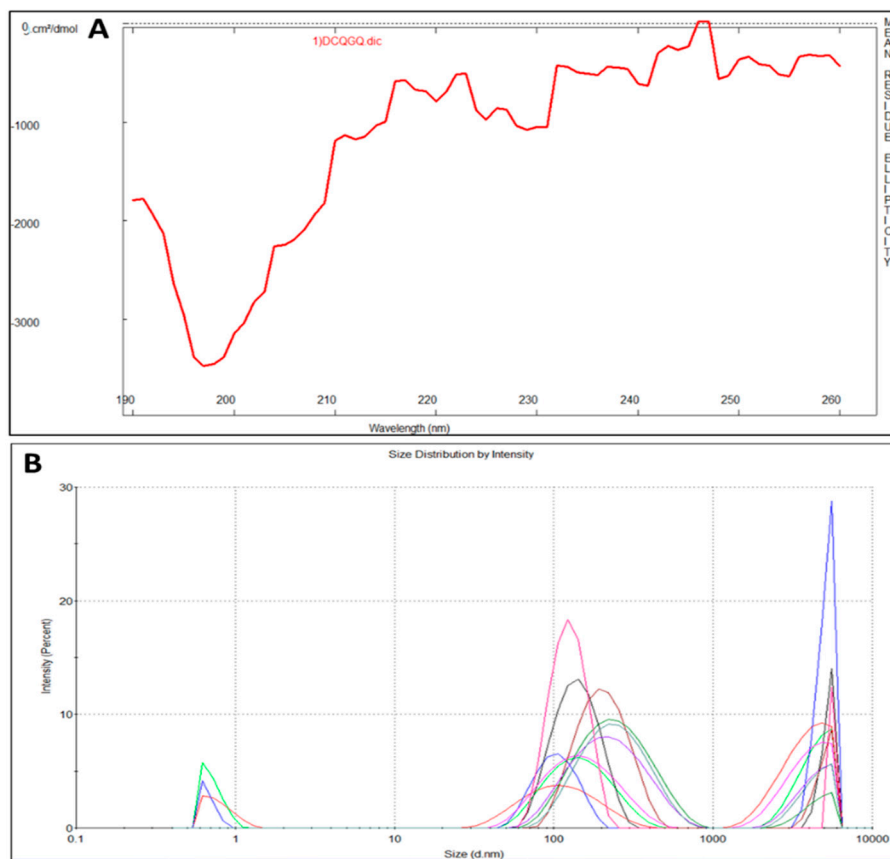


Figure 1. (A) Circular dichroism spectrum of cementum protein 1 C-terminal-derived synthetic peptide (CEMP1-p4). The lack of signals in the far UV region indicates that the peptide's secondary structure is mainly random-coiled. (B) Dynamic light scattering measurements revealed the CEMP1-p4 peptide adopts three oligomerization states at 37 °C.

2.2. CEMP1-p4 Induces Mineralization in a Cell-Free System

Scanning electron microscopy (SEM) analysis of the mineral formed in a semisolid gel in vitro by CEMP1-p4 revealed the formation of sphere-like structures with a size of $\sim 225 \mu\text{m}$ (Figure 2A). These spheres contained a core of disorganized small crystals. This core seemed to give origin to nascent needle-like crystals, which showed a radially spatial arrangement (Figure 2B) and became densely packed and changed to a quadrangular feature, ending angularly at the growing front (Figure 2C). The Ca/P ratio of the analyzed crystals by energy-dispersive X-ray spectroscopy (EDS) was of 1.52 ± 0.03 (spectrum inset in 2A), like hydroxyapatite's Ca/P ratio value in bone. Bovine serum albumin was used as a blank protein, which revealed that planar crystals were formed, and the deposited crystals resembled lamellae-like features. The crystals induced by BSA showed Ca/P ratio of 1.2 ± 0.06 (Figure 2D).

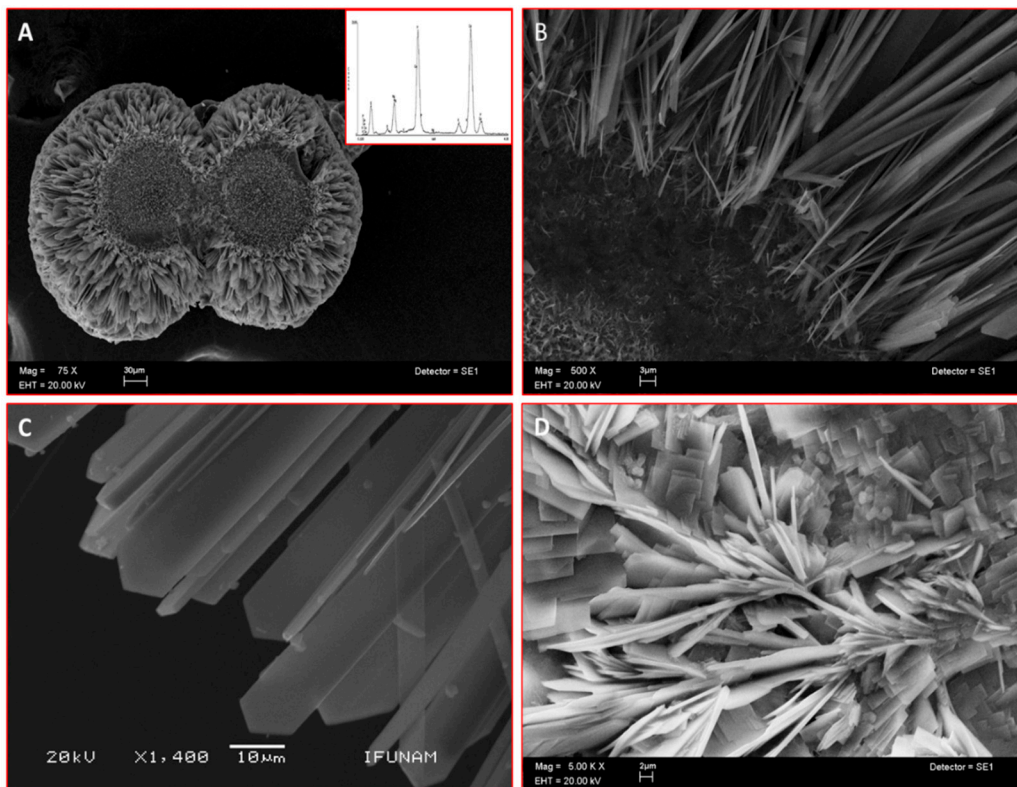


Figure 2. Scanning electron microscope (SEM) images of sphere-like structures formed in vitro by CEMP1-p4 (inset indicates Ca/P ratio of 1.52) (A). (B) Higher magnification shows an amorphous core with nascent needle-like crystals. (C) Hydroxyapatite crystals show a spear-like form. (D) Control crystals show irradiating crystals and plate-like crystals.

2.3. CEMP1-p4 Promotes Cell Proliferation

The cell proliferation assay demonstrated that CEMP1-p4 at a 4 $\mu\text{g/mL}$ was the optimal concentration, since HOMSCs proliferated by 83%, 92%, 101% and 113% at 24, 48, 72 and 96 h respectively when compared with positive controls (Figure 3A).

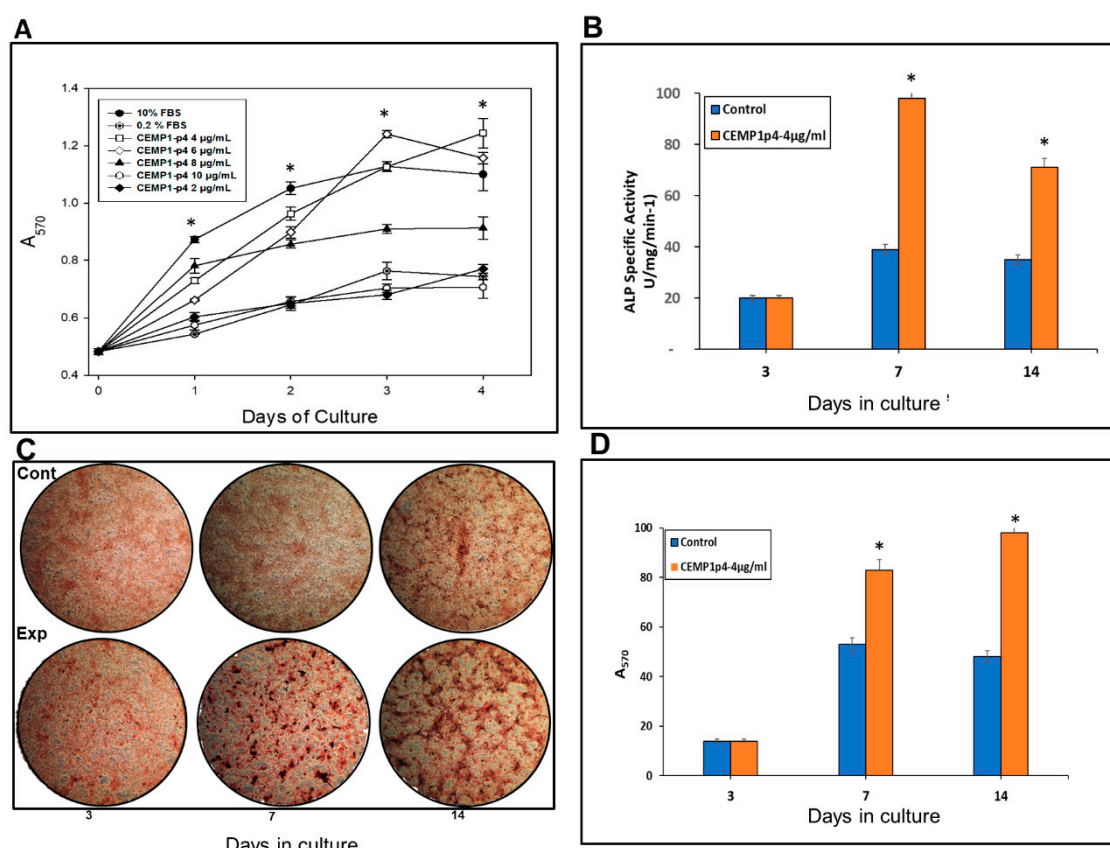


Figure 3. (A) Human oral mucosal stem cells (HOMSCs) were treated from 0 up to 96 h with several CEMP1-p4 concentrations where 4 µg/mL was shown to be optimal for cell proliferation. (B) CEMP1-p4 at 4 mg/mL increases alkaline phosphatase (ALP)-specific activity on HOMSCs at 7 and 14 days. (C) Representative images showing ARS after osteogenic induction on HOMSCs by CEMP1-p4 at 4 mg/mL during 3, 7, and 14 d of culture. (D) Mineral formation was quantified by cetylpyridinium chloride (CPC), showing that CEMP1-p4 is a potent inducer of calcium salts. * $p < 0.05$.

2.4. CEMP1-p4 Stimulated ALP Specific Activity by HOMSCs

HOMSCs treated with CEMP1-p4 at 4 µg/mL increased alkaline phosphatase-specific activity at 7 and 14 days by 1.5 and 1.1-fold respectively, when compared to controls (Figure 3B).

2.5. CEMP1-p4 induced HOMSCS's Mineralization

HOMSCs treated during 3, 7, and 14 days with CEMP1-p4 (4 µg/mL) showed that CEMP1-p4 induced HOMSCs to form mineralized calcium nodules. Control cells treated with 10% FBS supplemented with 5 mM β -glycerophosphate and 50 µg/mL ascorbic acid also formed calcium nodules (Figure 3C). However, mineral quantification demonstrated significant differences, since experimental cultures showed 58% and 107% increases on mineral deposits at 7 and 14 days of culture when compared to controls (Figure 3D).

2.6. Effect of CEMP1-p4 on Cell Signaling Pathway

2.6.1. CEMP1-p4 Induced mRNA Transcription of Wnt Signaling Pathway-Related Proteins

Activation of the canonical Wnt pathway has been described to affect proliferation and cell differentiation. At the mRNA level, CEMP1-p4 induces β -catenin relative expression by HOMSCs as early as 15 min after the addition of CEMP1-p4 by 6.6-fold, decreases at 30 and 60 min and increases by 2.1-fold at 2 h when compared to controls. Lef1 increases its expression by 2-fold at 30 min and Tcf1

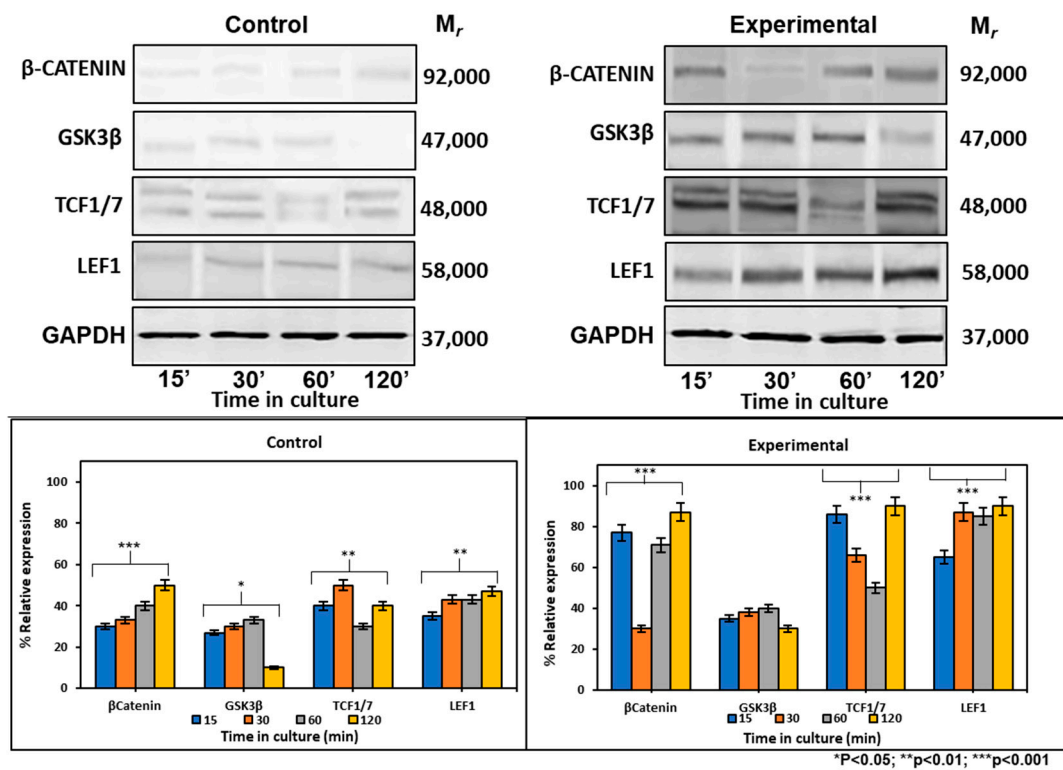


Figure 5. Expression of cell signaling pathway Wnt/ β -catenin-related markers at the protein level. Control cultures showed that β -catenin, GSK, TCF1/7 and LEF1 showed low expression at 15, 30, 60 and 120 min of culture. HOMSCs cultures treated with CEMP1-p4 at 4 μ g/mL increased β -catenin, TCF1/7 and LEF1 expression at 15, 30, 60 and 120 min respectively.

2.7. Expression of Mineralization-Related Markers at the mRNA and Protein Levels

Expression of mineralization-related markers at the mRNA level by HOMSCs at 3, 7 and 14 days revealed that at the initial stages of mineralization, RUNX2 and OSX increased by 2.1- and 3.7-fold and IBSP was barely expressed by 0.2-fold when compared to controls. At the middle stages of mineralization, OSX and IBSP increased its expression by 3.7- and 4.2-fold respectively, when compared to controls. OCN reached its maximum expression at late stages of mineralization by 1.7-fold when compared to controls. The results show that CEMP1-p4 promotes HOMSCs differentiation to a “mineralizing-like” cell phenotype (Figure 6).

data show that HOMSCs treated with CEMP1-p4 express osteoprogenitor markers and differentiate to a “mineralizing-like” cell phenotype.

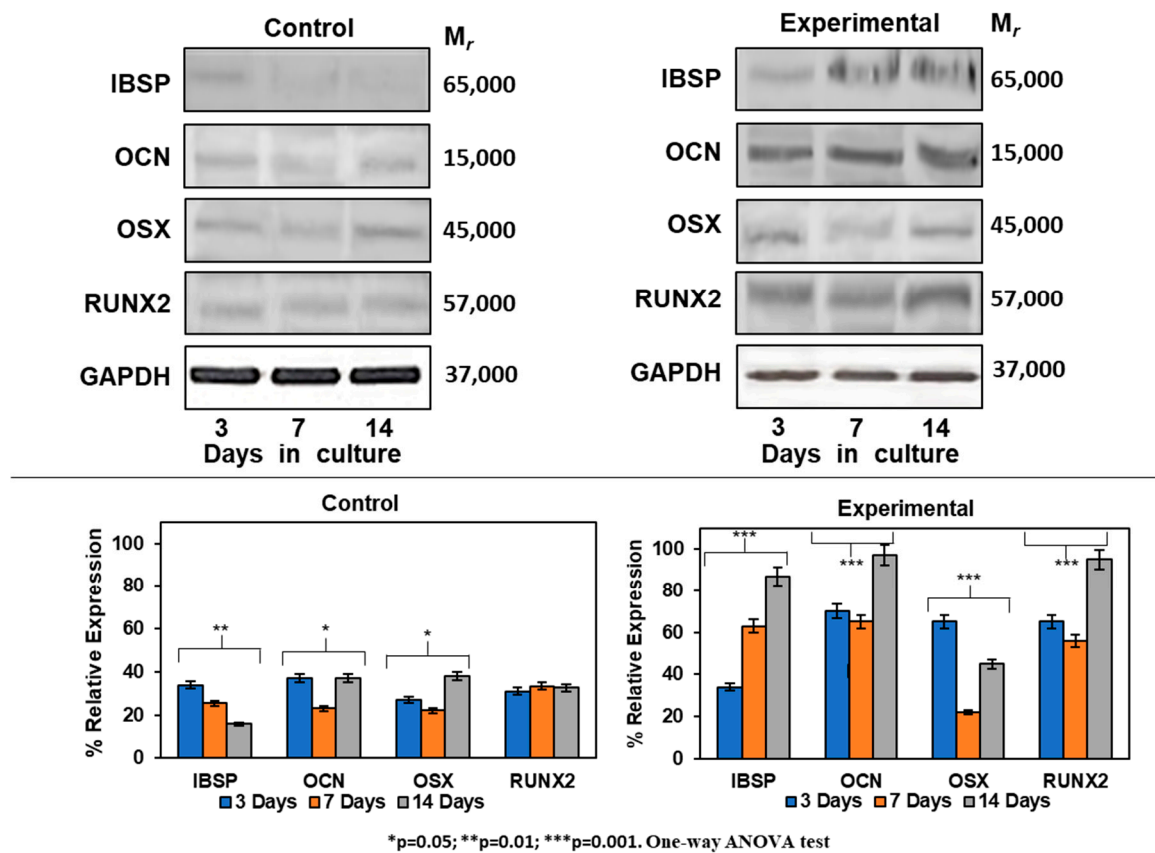


Figure 7. Expression of mineralization-related markers at the protein level. Experimental cultures treated with 4 $\mu\text{g/mL}$ showed a higher expression of IBSP, OSX, RUNX2 and OCN at all terms tested.

2.8. CEMP1-p4 was Internalized by HOMSCs

After 1 min, HOMSCs treated with CEMP1-p4 labelled with Alexa Fluor 546 showed spontaneous internalization with a nuclear and mostly perinuclear localization, with a compact and homogeneous distribution. After 1 and 15 min of incubation, CEMP1-p4 aggregates in the cytoplasm and maintained nuclear and perinuclear location. At 30 min, most of the peptide had agglomerated paranuclearly, with a few isolated aggregates in the nucleus. At 60 and 120 min, the peptide appeared to disperse and most of the fluorescent material had a diffuse localization around the nuclear area (Figure 8). These results revealed that CEMP1-p4 possessed several desired properties, such as solubility, rapid cell penetration and intracellular retention, and shows specific perinuclear and nuclear localization.

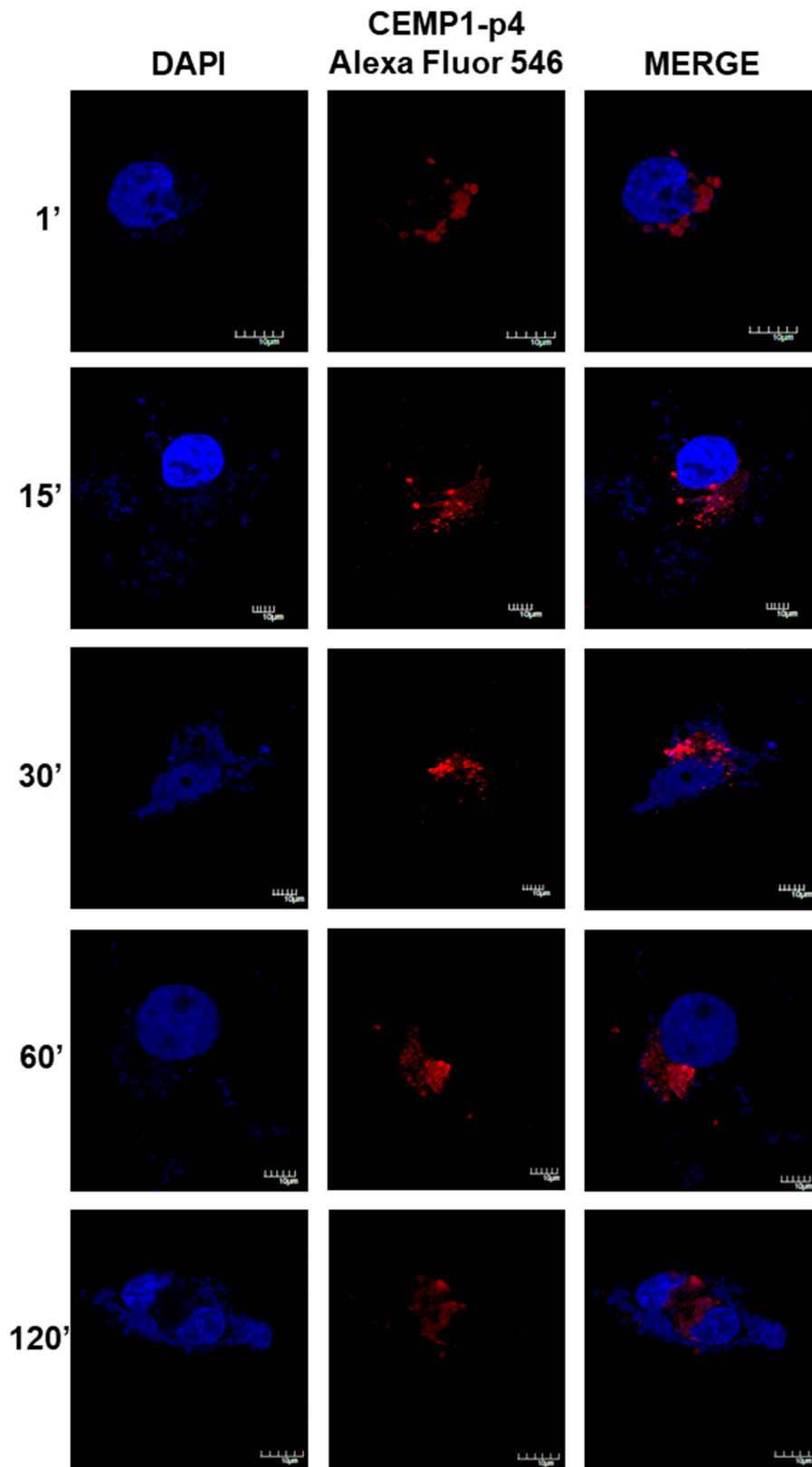


Figure 8. Confocal Microscopy Location of CEMP1-p4. CEMP1-p4 labelled with Alexa Fluor 546 was mainly located surrounding the nucleus from the first minute and the pattern was diffuse and organized into granules and dispersed at 120 min. Original magnification, 3400. Scale bar = 10 μ m.

2.9. β -Catenin Translocation by CEMP1-p4

Our results showed that after 15 min in the HOMSCs treated with CEMP1-p4, β -catenin expression was located surrounding the nuclear membrane, into the nucleus and cell membrane in a punctuate manner (Figure 9). At 1 hr, β -catenin's punctuate expression was more intense in the nucleus and cell cytoplasm. However, at 2 hrs after treatment, β -catenin almost disappeared from nucleus and was weakly located at the cell cytoplasm level (Figure 9).

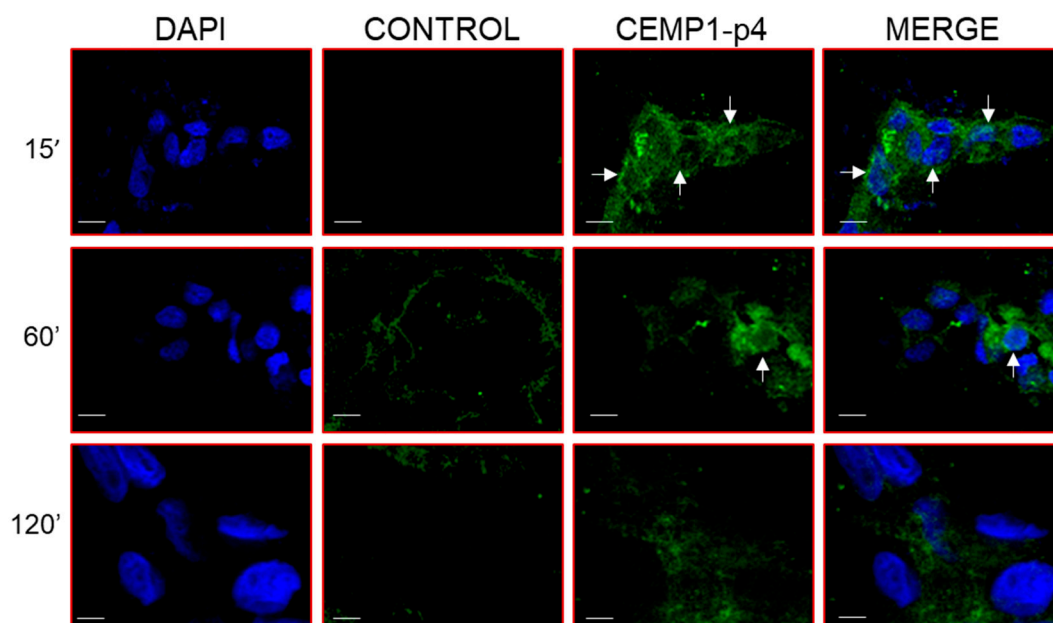


Figure 9. Translocation of β -catenin following HOMSC stimulation with CEMP1-p4 (4 $\mu\text{g}/\text{mL}$) was determined using antihuman β -catenin rabbit polyclonal antibody. Beta-catenin was localized in the cytoplasm from 15 up to 60 minutes. At 120 min after the treatment with CEMP1-p4, β -catenin began to be translocated into the nucleus. Image is representative of data from three independent experiments. Arrows indicate punctuate expression of β -catenin into the cell nucleus. Original magnification, 3400. Bar scale = 10 μm .

3. Discussion

The findings of this study show that a synthetic 15 amino acid-long peptide (CEMP1-p4), corresponding to CEMP1's C-terminus, activates β -catenin signaling in HOMSCs, inducing its differentiation to a “mineralizing-like” phenotype. This sequence shows 80% of intrinsic disorder-promoting amino acids in its composition. Therefore, it belongs to CEMP1's most intrinsic disordered region. The plasticity of the protein's N- and C-terminus regions show properties associated with crystal nucleation, growth and binding to hydroxyapatite crystals during the biomineralization process [20,21]. Our experimental data support this statement, since physicochemical characteristics of CEMP1-p4 revealed by circular dichroism showed that CEMP1-p4 has a random-coiled structure. DLS experimental data showed that CEMP1-p4 formed three different states of oligomerization—the monomer state with a hydrodynamic ratio of 0.5 nm, and two oligomers of 125 nm and 5.0 μm . DLS detected the peptide-peptide complex formation in a buffer solution, demonstrating for the first time a possible self-assembly ability.

CEMP1-p4 induces the formation of spheres with an amorphous calcium phosphate (ACP) center and has a significant effect on the mode of hydroxyapatite formation. The particles present in the center of the spheres eventually transformed to plate-like crystals, and due to its physicochemical properties, CEMP1-p4 induces hydroxyapatite crystal nucleation confirmed by EDS analyses that revealed a 1.52 Ca/P ratio. Acidic and disordered sequences accomplish several roles in crystal formation and controlling hydroxyapatite crystal growth. Indeed, peptides involved in biomineralization, such as

CEMP1-p4, have a random-coil secondary structure that allows intermolecular interactions at the peptide-mineral interface [22,23], probably by the interaction of CEMP1-p4 with phosphate ions caused by conformational changes in CEMP1-p4 that would promote the transformation of the amorphous phase to the crystalline phase [24].

Recently, mesenchymal stem cells isolated from the lamina propria of human oral mucosa [25,26] have shown to be multipotent and are able to differentiate into multilineage tissues, including bone, cartilage, adipose tissue, Schwann-like cells and neurons in vitro and in vivo [25,27–29]. Here, this study showed that HOMSCs treated with CEMP1-p4 increased their proliferation to a larger extent when compared with 10% FBS. We found that CEMP1-p4 triggers the expression of β -catenin as early as 15 min at the mRNA and protein level by 6.6- and 2.0-fold when compared with controls, respectively. It is also showed that CEMP1-p4 inactivates GSK-3 β , which increased the proliferation of HOMSCs, indicating that CEMP1-p4 possesses a growth factor-like activity. Because the β -catenin signaling pathway plays an important role during the mineralization process, we determined the expression of Gsk3b, Tcf1 and Lef1, which are fundamental to the Wnt/ β -catenin signaling pathway. Our results showed that CEMP1-p4 enhanced the expression of β -catenin, while expression of Gsk3b decreased and downstream transcriptional factors Tcf1 and Lef1 were activated by CEMP1-p4 treatment [30], revealing that CEMP1-p4 activated the Wnt/ β -catenin signaling pathway, inducing HOMSC differentiation to a “mineralizing-like” phenotype. More importantly, CEMP1-p4 appears to induce osteoprogenitor proliferation and differentiation by uncommitted HOMSCs. Gene expression at the mRNA and protein level of mineralization-related molecules further supports this premise [31]. At the mRNA level, RUNX2 was expressed at initial stages of mineralization. This transcriptional factor is of singular importance since it promotes the differentiation of osteoprogenitors to adopt a mature osteoblastic phenotype [32], meanwhile, OSX was expressed at the middle stages of mineralization. This transcriptional factor is associated with the regulation of bone formation [33]. Integrin-binding sialoprotein (IBSP) is a glycoprotein that plays important roles as a nucleator of hydroxyapatite crystals, cell attachment and cell differentiation [34–36]. CEMP1-p4 induced IBSP expression by HOMSCs at the middle stages of mineralization. OCN shows affinity for Ca²⁺ and regulates hydroxyapatite and participates in the late stages of mineralization [22,37,38]. Its expression implies the onset of mineralized matrix deposition. Significantly, at the protein level, CEMP1-p4 induces the strong expression of RUNX2 and OCN from 3 to 14 days when compared to controls. OSX was highly expressed at the initial and late stages of mineralization, and IBSP showed strong expression at the middle and late stages of mineralization. Increases in ALP activity by CEMP1-p4 and calcium nodule formation denotes that HOMSCs acquired a “mineralizing-like” phenotype [22,37,38]. These data taken together indicate that CEMP1-p4 leads HOMSCs to an osteoprogenitor cell phenotype through the Wnt/ β -catenin pathway. The differentiation of osteoprogenitors is under the regulation of various signaling pathways, a number of transcriptional factors that fundamentally determine the fate of stem cells toward a “mineralizing-like” phenotype [39–46]. Active Wnt signaling has been demonstrated to be required for conserving the pluripotency and proliferation of embryonic stem cells [16,17], as well as stem cell fate determination [47,48]. Wnt/ β -catenin is a principal pathway related to osteoblast differentiation [40,41,43,49–53], and it has been shown that in the presence of Wnt signaling, β -catenin accumulates in the cytoplasm and translocates into the nucleus, where it associates with Tcf/Lef transcription factors to regulate the expression of target genes [46,54–57]. β -catenin plays a direct role in osteoblast differentiation and some aspects of CEMP1-p4 may be mediated by β -catenin signaling [58–60]. However, β -catenin alone is not enough to induce osteogenic-like cell differentiation, unless other stimulatory signals are present [61]. We believe that one stimulatory factor is CEMP1-p4, since it promotes upregulation of RUNX2 expression [62]. This is supported by our findings, since β -catenin’s expression was located surrounding the nuclear membrane, in the nucleus and cell membrane as early as 15 min, and after 1 hr, β -catenin’s expression was more intense in the nucleus and cell cytoplasm. Our results indicate that CEMP1-p4 increases β -catenin expression, which make osteoprogenitor cells capable of differentiating to osteoblasts [39,63]

Peptides show a propensity to bind flat protein surfaces, however, most peptides are incapable of passing through the cell membrane and therefore, their usefulness is limited. Cell-penetrating peptides (CPPs) either contain mainly positively charged amino acids or an alternating pattern of charged and hydrophobic side chains [64,65]. Hydrophobicity is crucial for bilayer insertion and penetration, as hydrophobic amino acids interact with the core of membranes [66–68]. Using confocal microscopy, we examined the subcellular location of fluorescein-labelled CEMP1-p4. The peptide showed a perinuclear localization as early as 1 min after its addition to the medium. The CEMP1-p4 peptide organized into homogeneous aggregates, adopting a paranuclear localization and a few aggregates in the nucleus. As the time advanced, CEMP1-p4 accumulated into vesicular structures, possibly endosomes [69]. Some characteristics are necessary for efficient cell uptake of CPPs: a) hydrophobicity to a certain degree; and b) stretches of hydrophobic and cationic amino acids. Cemp1-p4 possesses these characteristics and could be the reason why the peptide penetrated the cell membrane and adopted a paranuclear location only one min after its addition. This is crucial for the activation of the Wnt pathway [70–73] and of clinical relevance, since bioactive and cell-permeable peptides represent a promising strategy for the application of peptide-derived drugs. Our findings of β -catenin signaling in HOMSCs and its stimulation by CEMP1-p4 might have potential therapeutic implications for the repair and regeneration of mineralized tissues including bone, cementum and dentin.

4. Materials and Methods

4.1. Peptide Synthesis

A sequence corresponding to human cementum protein 1 (CEMP1; Accession: NP_001041677.1; GI: 115292438), C-terminal domain with an amino acid sequence QGQGDTEDEGRMTLMG (CEMP1-p4); corresponding to 233–247 aa was synthesized by solid phase techniques (Fmoc). Then, C-18 reversed-phase liquid chromatography purification was performed up to 95% (New England Peptide, Ipswich, MA, USA). The lyophilized peptide was dissolved in distilled deionized water and filtered (0.22 μ m filter) before use.

4.2. Characterization of CEMP1-p4 Synthetic Peptide

To determine if CEMP1-p4 possessed a secondary structure, the peptide was analyzed by circular dichroism spectroscopy (CD) and its behavior in solution was analyzed by dynamic light scattering (DLS).

4.3. Circular Dichroism

Synthetic CEMP1-p4 was dissolved in 10 mM sodium phosphate buffer, pH 7.4 at 200 μ g/mL concentration. CD spectra were collected using a JASCO J-710 spectropolarimeter (cell length = 1 mm). CD data were collected from 190–260 nm. A baseline 10 mM sodium phosphate, pH 7.4 buffer solution was recorded separately and subtracted from each spectrum. CD data were analyzed by the program Dicroprot to determine CEMP1-p4' secondary structure with the Hennessey & Johnson algorithm [74].

4.4. Dynamic Light Scattering

Measurements of the CEMP1-p4 solution were acquired with a Zetasizer Nano S (Malvern Instruments, Ltd., Clevedon Organs, UK) molecular sizing instrument [75]. The temperature was held at 37 (0.1 $^{\circ}$ C) with a Peltier unit. Data analyses were performed using the software Zetasizer Nano Family age (V.7.10), (Malvern Instruments, Ltd., Clevedon Organs, UK).

In silico analyses—the isoelectric point (pI), molecular weight, hydrophobic character and GRAVY of the CEMP1-p4 peptide were determined by using the ExPASy tool ProtParam. (<https://web.expasy.org/protparam/>).

4.5. Mineralization in a Cell-Free System

Calcium phosphate crystal formation was induced by CEMP1-p4 in a cell-free system, which consisted of a semisolid medium at physiological pH at RT (room temperature) as described elsewhere (Montoya et al. 2014). Briefly, a sodium metasilicate (SMS) solution of specific gravity 1.06 g/mL, 1 M H₃PO₄, HEPES buffer 10 mM, pH 7.2 was used. CEMP1-p4 peptide (10 µg/mL) was dissolved in 10 mM HEPES pH 7.4 and mixed with the SMS. After gel formation, 100 mM CaCl₂ in 10 mM HEPES buffer, pH 7.4, was added over the crystallizing medium. Gels were incubated at 37 °C for 7 days. Bovine serum albumin (20 µg/mL) was used as a negative control. Elemental chemical composition and morphology of the crystals were performed by scanning electron microscopy (JSM 5600LV; JEOL USA Inc., Peabody, MA, USA). The calcium to phosphate ratio (Ca/P) was obtained by the energy-dispersive X-ray spectroscopy (EDS) analysis (Noran X-ray microanalysis detector, model Voyager 4.2.3; Thermo Scientific, Waltham, MA, USA). Once the composition was obtained, the crystals were covered with a 100 nm thick gold film.

4.6. Cell Culture

HOMSCS were isolated and grown as described elsewhere [6]. Human tissue from the oral mucosa was obtained from donors that underwent routine oral surgery procedures. The protocol was reviewed and approved by the Ethics Committee at the National University of Mexico School of Dentistry (UNAM), 9 March 2018; Register # CIE/0303/02/2018. For the experiment, cells between the 2nd and 5th passages were used. HOMSCs were maintained in DMEM supplemented with 10% fetal bovine serum (FBS; Thermo Fisher Scientific, Waltham, MA, USA), and antibiotics (penicillin 10 UI/mL, streptomycin: 100 µg/mL), and cultured in 5% CO₂ and 95% air atmosphere with 100% humidity. Mineralizing media (MM), consisting of materials described above plus 5 mM β-glycerophosphate, ascorbic acid (50 µg/mL) and dexamethasone (10⁻⁷ M), was used.

4.7. Cell Proliferation Assay

The effect of CEMP1-p4 on proliferation was performed by using the colorimetric MTT assay 3-(4,5-dimethylthazol-2-yl)-2,5-diphenyl tetrazolium bromide (Boehringer Mannheim, Indianapolis, IN, USA). HOMSCs were plated at 0.5 × 10⁴ density in 96-well plates (Thermo Fisher Scientific). After overnight attachment, experimental cells were treated from 0 up to 96 h with several CEMP1-p4 concentrations (0, 2, 4, 6, 8 and 10 µg/mL) in medium containing 0.2% FBS. Control cells without CEMP-1-p4 treatment were cultured in the presence of 10% FBS (positive control), or in presence of 0.2% FBS alone (negative control). At the end of the treatment intervals (every 24 h), MTT solution (5 mg/mL) in PBS was added to the wells and incubated at 37 °C for 4 h. Lysing buffer (20% sodium dodecyl sulfate, 50% dimethyl formamide (pH 4.7) was added to each well and plates were incubated for 1 h at 37 °C. The resultant solution was read at 570 nm on a microplate reader (Filter Max F5; Molecular Devices, Sunnyvale, CA, USA).

4.8. Time Course Experiments

To identify the signal transduction pathways involved in the regulation of gene expression by CEMP1-p4 at the mRNA and protein levels, HOMSCs cells were plated at 5 × 10⁴ density in 6-well culture plates and culture conditions were as follows—1) 0.2% FBS plus 4.0 µg/mL of CEMP1-p4 (experimental), and 0.2% FBS alone (negative control) and 10% FBS (positive control). The CEMP1-p4 dose was selected according to the previous findings from the dose-response on cell proliferation. Total RNA and proteins were extracted at 0', 15', 30', 60' and 120' after treatment. At the mRNA and protein level, the expression of β-catenin, Gsk3b, Tcf1 and Lef1 was performed.

4.9. HOMSC Mineralization

In order to determine the effect of CEMP1-p4 on the induction of the mineralization process *in vitro*, HOMSCs were plated at 5×10^4 density in 6-well plates (Thermo Fisher Scientific, CDMX, Mexico) and allowed to attach overnight. Cells were cultured for 5, 10 and 15 days under the following conditions—10% FBS plus 3 mM β -glycerophosphate and 50 mg/mL ascorbic acid (controls) or with 4 μ g/mL of CEMP1-p4 (experimental).

4.10. Alkaline Phosphatase Activity

HOMSCs were plated at 5×10^4 density in 6-well culture plates and cultured for 5, 10 and 15 days in the conditions as previously described [12]. Alkaline phosphatase (ALP)-specific activity was performed as described by Lowry et al. [76]. The activity was expressed as nanomoles of p-nitrophenol per minute per milligram of protein. Protein content was determined as described elsewhere [77].

4.11. Alizarin Red Staining and Quantification of Mineralization

HOMSCs were plated at a density of 5×10^4 cells, in 6-well plates (Thermo Fisher Scientific) in the conditions described above. Culture medium was replaced every other day and cells were fixed with 4% paraformaldehyde and rinsed with PBS. Cultures were stained with 2% Alizarin Red S at pH 4.2 (ARS; Millipore Sigma, Burlington, MA, USA) for 10 min. Calcium deposits were documented and analyzed with ImageJ software (National Institutes of Health (NIH), Bethesda, MD, USA) Mineralization was quantified by the cetylpyridinium chloride (CPC) method [12]. Briefly, alizarin red was diluted in a 2 mL/well with 10% CPC, and incubated for 1 h at 37 °C. Then, the solution was diluted five times in CPC, and the absorbance reading was at 570 nm (Filter Max F5; Molecular Devices, LLC. San Jose, CA, USA). Experiments were performed in triplicate and repeated twice.

4.12. Real-Time Quantitative RT-PCR

HOMSCs were cultured under conditions as described above for 5, 10, and 15 d. Cells were collected and total RNA was extracted with Trizol Reagent (Thermo Fisher Scientific, Waltham, MA, USA). Ten RNA nanograms were used per reaction, and the level of mRNA expression was quantified by the one-step real-time quantitative RT-PCR (RT-qPCR) method using Super-Script III Platinum Sybr Green One-Step qPCR Kit (Thermo Fisher Scientific). The conditions for a 25 μ L reaction were as follows—cDNA synthesis at 50 °C for 3 min, denaturation at 95 °C for 5 min; thereafter 40 cycles of 95 °C for 15 s, 60 °C for 30 s, and a 40 °C hold cycle for 1 min. Reactions were performed in a Corbett Rotor-Gene 6000 (Qiagen, Germantown, MD, USA). Primer sequences for human genes encoding IBSP, OCN, runt-related transcription factor-2 (RUNX)-2, osterix (OSX), β -catenin, Gsk3b, Tcf1, Lef1 and glyceraldehyde 3-phosphatedehydrogenase (GAPDH) are shown in Table 1.

Table 1. Primers Used for RT-qPCR.

Gene	Primer Sequence 5'-3'	
	Forward	Reverse
β -CATENIN	GGTGCTGACTATCCAGTTG	GGCAGAGTAAAGTATTCACCC
GSK3 β	GACTTTGGAAGTGCAAAGC	AGGAAATATTGGTTGTCCTAGC
LEF1	GAAGAGGAGGGCGACTTAG	CTTTCCTTCATCAGGGTGTTTC
TCF1	CCAACATTCTCAGGTCCG	GAGCAAGCCAGGTGTTC
IBSP	AACGAAGAAAGCGAAGCAGAA	TCTGCCTCTGTGCTGTTGGT
OCN	GTTGCAGGCTCAATCCATT	CCATCCTCATACTGCACCT
OSX	GCCAGAAGCTGTGAAACCTC	GCTGCAAGCTCTCCATAACC
RUNX2	ACCCAGAAGGCACAGACAGAAG	AGGAATCGCCCCTAAATCACT
GAPDH	CAACGGATTGGTCGTATTGG	GCAACAATATCCACTTTACCAGAGTTAA

4.13. Western Blot Analysis

HOMSCs were plated at 5×10^4 density in 6-well culture plates. Culture conditions were as described above and cells cultured for 5, 10, and 15 d. At the end of each term, the cells were scraped with a policeman and dissolved in lysis buffer containing 1% SDS and a protease inhibitor cocktail [7]. Western blots were performed with rabbit polyclonal antibodies against human OSX, RUNX2, OCN, CEMP1, CAP, GAPDH, and a monoclonal antibody against human IBSP, (Santa Cruz Biotechnology, Dallas, TX, USA), WNT3 α , GSK-3 β , β -catenin, Tcf and Lef1 (Jackson Immuno Research Lab, Inc. West Grove, PA, USA). Proteins from experimental and control groups (20 mg/lane) were separated on a 12% SDS-PAGE and electroblotted onto a PVDF membrane (Immobilon-P; Millipore Sigma). Membranes were blocked with 5% nonfat milk for 1 h and then incubated with 1:1000 diluted antibodies for 1 h, then washed with PBS three times. After they were washed, the membranes were incubated with 1:1000 diluted horseradish peroxidase-conjugated goat antirabbit, or goat antimouse IgG secondary antibodies for 1 h. Membranes were washed with PBS and developed as described elsewhere [7]. For assessment of the Western blot, all membranes were digitalized with an Epson V550 scanner and processed and analyzed with ImageJ software (National Institutes of Health (NIH), Bethesda, MD, USA). The relative level of each protein was assessed by measuring the integrated intensity of all pixels in each band, excluding the local background. Results are expressed as percentages of protein intensity.

4.14. Confocal Microscopy Analysis

In order to determine CEMP1-p4 internalization and location, HOMSCs were plated at 0.5×10^3 in Lab-Tek chamber slides. Cells were cultured overnight and incubated for 1, 15, 30, 60 and 120 min with CEMP1-p4 labelled with Alexa Fluor 546, as described elsewhere [24]. Fluorescence images were obtained using an Olympus FV1000 confocal laser scanning microscope (Olympus America, CDMX, México) fitted with a $\times 20$ objective lens. Control cells were incubated with Alexa 546 alone. Images were analyzed using the plot profile option in ImageJ.

4.15. Immunofluorescence

HOMSCs treated with CEMP1-p4 at 4 $\mu\text{g}/\text{mL}$ were incubated for 15, 60 and 120 min, then fixed in 4% paraformaldehyde for 10 min at RT, incubated overnight at 4 °C with a Moab to β -catenin (BD Biosciences, San Jose, CA, USA). For nuclear localization analysis, the fixed samples were subjected to fluorescent digital confocal imaging analysis using a Zeiss LSM 510 confocal microscope (Carl Zeiss, CDMX, México).

5. Conclusions

This study shows for the first time the involvement of the Wnt/ β -catenin signaling pathway in CEMP1-p4-mediated differentiation in HOMSCs. The role of a CEMP1-p4 suggests that the intracellular mechanism associated with the activation of trigger genes to induce stem cell differentiation towards an osteoblastic phenotype is through the activity of the molecules of the canonical Wnt/ β -catenin signaling pathway induced by CEMP1-p4. However, it is still necessary to know the mechanism of interaction of this peptide with these molecules that allow for recognition if it is through interactions by phosphorylation that allow for activating or inactivating of molecular complexes associated with this pathway.

Author Contributions: Conceptualization, H.A. and Y.G.; methodology, R.A., E.R., C.P. and L.H.; formal analysis, R.A., and S.L.; resources, H.A., G.M. and L.H.; data curation, S.L. and C.P.; writing—original draft preparation, R.A. and G.M.; writing—review and editing, H.A., Y.G, S.L. and E.R. All authors have read and agreed to the published version of the manuscript.

Acknowledgments: The authors are grateful for support from DGAPA-UNAM-IT200717, Programa de Maestría y Doctorado en Ciencias Médicas, Odontológicas y de la Salud (PMDCMOS-UNAM). Rita Arroyo acknowledges financial support by the Consejo Nacional de Ciencia y Tecnología, México, (CVU: 420475) and Dr. Karina Jiménez, USAII, Facultad de Química, UNAM.

Conflicts of Interest: The authors declare no conflict of interest.

Abbreviations

CAP	Cementum Attachment Protein
CEMP1	Cementum Protein 1
CEMP1-p4	Cementum Protein1-Peptide 4
CD	Circular Dichroism
CPC	Cetylpyridinium Chloride
CPPs	Cell Penetrating Peptides
DMEM	Dulbecco's Modified Eagle Medium
DLS	Dynamic Light Scattering
EDS	Energy Dispersive X ray spectroscopy
FBS	Fetal Bovine Serum
Fmoc	Fluorenylmethyloxycarbonyl
GAPDH	Glyceraldehyde-3-Phosphate Dehydrogenase
GRAVY	Grand Average of Hydropathicity
GSK3 β	Glycogen synthase kinase 3 beta
HA	Hydroxyapatite
HEPES	2-[4-(2-hydroxyethyl) piperazin-1-yl] ethanesulfonic acid
HOMSCs	Human Oral Mucosa Stem Cells
IBSP	Integrin Bone Sialoprotein
IDP	Intrinsically Disordered Protein
LEF1	Lymphoid Enhancer binding Factor 1
MTT	3-(4,5-dimethylthiazol-2-yl)-2,5-diphenyltetrazolium bromide
OCN	Osteocalcin
OSX	Osterix
RUNX2	Core-Binding Factor Subunit Alpha-1
RPLC	Reverse-Phase Liquid Chromatography
SEM	Scanning Electron Microscopy
SMS	Sodium Metasilicate
TCF	T-cell transcription Factor
Wnt	Wingless-related integration site

References

1. Tonetti, M.S.; Jepsen, S.; Jin, L.; Otomo-Corgel, J. Impact of the global burden of periodontal diseases on health, nutrition and wellbeing of mankind: A call for global action. *J. Clin. Periodontol.* **2017**, *44*, 456–462. [[CrossRef](#)]
2. Arzate, H.; Zeichner-David, M.; Mercado-Celis, G. Cementum proteins: role in cementogenesis, biomineralization, periodontium formation and regeneration. *Periodontol 2000* **2015**, *67*, 211–233. [[CrossRef](#)]
3. King, G.N. New regenerative technologies: Rationale and potential for periodontal regeneration: 1. New advances in established regenerative strategies. *Dent. Update* **2017**, *28*, 7–12. [[CrossRef](#)] [[PubMed](#)]
4. King, G.N. New regenerative technologies: Rationale and potential for periodontal regeneration: 2. Growth factors. *Dent. Update* **2017**, *28*, 60–65. [[CrossRef](#)] [[PubMed](#)]
5. King, G.N.; Cochran, D.L. Factors that modulate the effects of bone morphogenetic protein-induced periodontal Cementum proteins 229 regeneration: a critical review. *J. Periodontol.* **2002**, *73*, 925–936. [[CrossRef](#)] [[PubMed](#)]
6. Treves-Manusevitz, S.; Hoz, L.; Rachima, H.; Montoya, G.; Tzur, E.; Vardimon, A.; Narayanan, A.S.; Amar, S.; Arzate, H.; Pitaru, S. Stem cells of the lamina propria of human oral mucosa and gingiva develop into mineralized tissues in vivo. *J. Clin. Periodontol.* **2013**, *40*, 73–81. [[CrossRef](#)] [[PubMed](#)]
7. Alvarez, M.; Narayanan, S.; Zeichner-David, M.; Carmona, B.; Arzate, H. Molecular cloning, expression and immunolocalization of a novel human cementum-derived protein (CP-23). *Bone* **2006**, *38*, 409–419. [[CrossRef](#)]
8. Valdés De Hoyos, A.; Hoz-Rodríguez, L.; Arzate, H.; Narayanan, A.S. Isolation of protein-tyrosine phosphatase-like member-a variant from cementum. *J. Dent. Res.* **2012**, *91*, 203–209. [[CrossRef](#)]

9. Hoz, L.; Romo, E.; Zeichner-David, M.; Sanz, M.; Nuñez, J.; Gaitán, L.; Mercado, G.; Arzate, H. Cementum protein 1 (CEMP1) induces differentiation by human periodontal ligament cells under three-dimensional culture conditions. *Cell Biol. Int.* **2012**, *36*, 129–136. [[CrossRef](#)]
10. Nuñez, J.; Sanz-Blasco, S.; Vignoletti, F.; Muñoz, F.; Arzate, H.; Villalobos, C.; Nuñez, L.; Caffesse, R.G.; Sanz, M. Periodontal regeneration following implantation of cementum and periodontal ligament-derived cells. *J. Periodontol. Res.* **2012**, *47*, 33–44. [[CrossRef](#)]
11. Komaki, M.; Iwasaki, K.; Arzate, H.; Narayanan, A.S.; Izumi, Y.; Morita, I. Cementum protein 1 (CEMP1) induces a cementoblastic phenotype and reduces osteoblastic differentiation in periodontal ligament cells. *J. Cell Physiol.* **2012**, *227*, 649–657. [[CrossRef](#)] [[PubMed](#)]
12. Correa, R.; Arenas, J.; Montoya, G.; Hoz, L.; López, S.; Salgado, F.; Arroyo, R.; Salmeron, N.; Romo, E.; Zeichner-David, M.; et al. Synthetic cementum protein 1-derived peptide regulates mineralization in vitro and promotes bone regeneration in vivo. *FASEB J.* **2019**, *33*, 1167–1178. [[CrossRef](#)] [[PubMed](#)]
13. Gordon, M.D.; Nusse, R. Wnt signaling: Multiple pathways, multiple receptors, and multiple transcription factors. *J. Biol. Chem.* **2006**, *281*, 22429–22433. [[CrossRef](#)] [[PubMed](#)]
14. Moon, R.T.; Kohn, A.D.; De Ferrari, G.V.; Kaykas, A. WNT and beta-catenin signalling: Diseases and therapies. *Nat. Rev. Genet.* **2004**, *5*, 691–701. [[CrossRef](#)] [[PubMed](#)]
15. Stadel, R.; Hoffmann, R.; Basler, K. Transcription under the control of nuclear Arm/beta-catenin. *Curr. Biol.* **2006**, *16*, R378–R385. [[CrossRef](#)]
16. Feng, Z.; Srivastava, A.S.; Mishra, R.; Carrie, E.A. Regulatory role of Wnt signaling pathway in the hematopoietic differentiation of murine embryonic stem cells. *Biochem. Biophys. Res. Commun.* **2004**, *324*, 1333–1339. [[CrossRef](#)]
17. Sato, N.; Meijer, L.; Skaltsounis, L.; Greengard, P.; Brivanlou, A.H. Maintenance of pluripotency in human and mouse embryonic stem cells through activation of Wnt signaling by a pharmacological GSK-3-specific inhibitor. *Nat. Med.* **2004**, *10*, 55–63. [[CrossRef](#)]
18. Liu, Z.; Habener, J.F. Glucagon-like Peptide-1 Activation of TCF7L2-dependent Wnt Signaling Enhances Pancreatic Beta Cell Proliferation. *J Biol Chem.* **2008**, *283*, 8723–8735. [[CrossRef](#)]
19. Willert, K.; Jones, K.A. Wnt signaling: Is the party in the nucleus? *Genes Dev.* **2006**, *20*, 1394–1404. [[CrossRef](#)]
20. Evans, J.S. “Tuning in” to mollusk shell nacre- and prismatic-associated protein terminal sequences. Implications for biomineralization and the construction of high-performance inorganic-organic composites. *Chem Rev.* **2008**, *108*, 4455–4462. [[CrossRef](#)]
21. Nudelman, F.; Chen, H.H.; Goldberg, H.A.; Weiner, S.; Addadi, L. Spiers Memorial Lecture Lessons from biomineralization: comparing the growth strategies of mollusk shell prismatic and nacreous layers in *Atrina rigida*. *Faraday Discuss.* **2007**, *136*, 9–25. [[CrossRef](#)] [[PubMed](#)]
22. Komori, T. Regulation of osteoblast differentiation by transcription factors. *J. Cell Biochem.* **2006**, *99*, 1233–1239. [[CrossRef](#)] [[PubMed](#)]
23. Choi, J.W.; Jeong, W.S.; Yang, S.J.; Park, E.J.; Oh, T.S.; Koh, K.S. Appropriate and effective dosage of BMP-2 for the ideal regeneration of calvarial bone defects in beagles. *Plast Reconstr. Surg.* **2016**, *138*, 64e–72e. [[CrossRef](#)] [[PubMed](#)]
24. Montoya, G.; Correa, R.; Arenas, J.; Hoz, L.; Romo, E.; Arroyo, R.; Zeichner-David, M.; Arzate, H. Cementum protein 1-derived peptide (CEMP 1-p1) modulates hydroxyapatite crystal formation in vitro. *J. Pept. Sci.* **2019**, *25*, e3211. [[CrossRef](#)]
25. Carstanjen, B.; Desbois, C.; Hekmati, M.; Behr, L. Successful engraftment of cultured autologous mesenchymal stem cells in a surgically repaired soft palate defect in an adult horse. *Can. J. Vet. Res.* **2006**, *70*, 143–147.
26. Bergman, R.J.; Gazit, D.; Kahn, A.J.; Gruber, H.; McDougall, S.; Hahn, T.J. Age-related changes in osteogenic stem cells in mice. *J. Bone Miner. Res.* **1996**, *11*, 568–577. [[CrossRef](#)]
27. Grigoriadis, A.E.; Heersche, J.N.; Aubin, J.E. Differentiation of muscle, fat, cartilage, and bone from progenitor cells present in a bone-derived clonal cell population: effect of dexamethasone. *J. Cell Biol.* **1988**, *106*, 2139–2151. [[CrossRef](#)]
28. Johnstone, B.; Hering, T.M.; Caplan, A.I.; Goldberg, V.M.; Yoo, J.U. In vitro chondrogenesis of bone marrow-derived mesenchymal progenitor cells. *Exp. Cell Res.* **1998**, *238*, 265–272. [[CrossRef](#)]
29. Kadiyala, S.; Young, R.G.; Thiede, M.A.; Bruder, S.P. Culture expanded canine mesenchymal stem cells possess osteochondrogenic potential in vivo and in vitro. *Cell Transplant.* **1997**, *6*, 125–134. [[CrossRef](#)]

30. Zhang, H.; Li, H. Tricin enhances osteoblastogenesis through the regulation of Wnt/ β -catenin signaling in human mesenchymal stem cells. *Mech Dev.* **2018**, *152*, 38–43. [[CrossRef](#)]
31. De Boer, J.; Wang, H.J.; Van Blitterswijk, C. Effects of Wnt signaling on proliferation and differentiation of human mesenchymal stem cells. *Tissue Eng.* **2004**, *10*, 393–401. [[CrossRef](#)] [[PubMed](#)]
32. Zhang, Y.; Xie, R.L.; Croce, C.M.; Stein, J.L.; Lian, J.B.; van Wijnen, A.J.; Stein, G.S. A program of microRNAs controls osteogenic lineage progression by targeting transcription factor Runx2. *Proc. Natl. Acad. Sci. USA.* **2011**, *108*, 9863–9868. [[CrossRef](#)] [[PubMed](#)]
33. Sun, S.; Wang, Z.; Hao, Y. Osterix overexpression enhances osteoblast differentiation of muscle satellite cells in vitro. *Int. J. Oral Maxillofac. Surg.* **2008**, *37*, 350–356. [[CrossRef](#)] [[PubMed](#)]
34. Chen, J.K.; Shapiro, H.S.; Wrana, J.L.; Reimers, S.; Heersche, J.N.; Sodek, J. Localization of bone sialoprotein (BSP) expression to sites of mineralized tissue formation in fetal rat tissues by in situ hybridization. *Matrix* **1991**, *11*, 133–143. [[CrossRef](#)]
35. Hunter, G.K.; Goldberg, H.A. Nucleation of hydroxyapatite by bone sialoprotein. *Proc. Natl. Acad. Sci. USA.* **1993**, *90*, 8562–8565. [[CrossRef](#)]
36. Hunter, G.K.; Hauschka, P.V.; Poole, R.A.; Rosenberg, L.C.; Goldberg, H.A. Nucleation and inhibition of Hydroxyapatite formation by mineralized tissue proteins. *Biochem. J.* **1996**, *317*, 59–64. [[CrossRef](#)]
37. Hough, T.A.; Polewski, M.; Johnson, K.; Cheeseman, M.; Nolan, P.M.; Vizer, L.; Rastan, S.; Boyde, A.; Pritzker, K.; Hunter, A.J.; et al. Novel mouse model of autosomal semi dominant adult hypophosphatasia has a splice site mutation in the tissue nonspecific alkaline phosphatase gene Akp2. *J. Bone Miner. Res.* **2007**, *22*, 1397–1407. [[CrossRef](#)]
38. Thomas, G.P.; Baker, S.U.; Eisman, J.A.; Gardiner, E.M. Changing RANKL/OPG mRNA expression in differentiating murine primary osteoblasts. *J. Endocrinol.* **2002**, *170*, 451–460. [[CrossRef](#)]
39. Tang, N.; Song, W.X.; Luo, J.; Luo, X.; Chen, J.; Sharff, K.A.; Bi, Y.; He, B.C.; Huang, J.Y.; Zhu, G.H.; et al. BMP-9 induced osteogenic differentiation of mesenchymal progenitors requires functional canonical Wnt/ β -catenin signalling. *J. Cell Mol. Med.* **2009**, *13*, 2448–2464. [[CrossRef](#)]
40. Deng, Z.L.; Sharff, K.A.; Tang, N.; Song, W.X.; Luo, J.; Luo, X.; Chen, X.; Bennett, E.; Reid, R.; Manning, D.; et al. Regulation of osteogenic differentiation during skeletal development. *Front. Biosci.* **2008**, *13*, 2001–2021. [[CrossRef](#)]
41. Karsenty, G.; Wagner, E.F. Reaching a genetic and molecular understanding of skeletal development. *Dev. Cell* **2002**, *2*, 389–406. [[CrossRef](#)]
42. Molofsky, A.V.; Pardal, R.; Morrison, S.J. Diverse mechanisms regulate stem cell self-renewal. *Curr. Opin. Cell Biol.* **2004**, *16*, 700–707. [[CrossRef](#)] [[PubMed](#)]
43. Wang, J.; Wynshaw-Boris, A. The canonical Wnt pathway in early mammalian embryogenesis and stem cell maintenance/ differentiation. *Curr. Opin. Genet. Dev.* **2004**, *14*, 533–539. [[CrossRef](#)] [[PubMed](#)]
44. Kleber, M.; Sommer, L. Wnt signaling and the regulation of stem cell function. *Curr. Opin. Cell Biol.* **2004**, *16*, 681–687. [[CrossRef](#)]
45. Reya, T.; Clevers, H. Wnt signalling in stem cells and cancer. *Nature* **2005**, *434*, 843–850. [[CrossRef](#)]
46. Luo, J.; Chen, J.; Deng, Z.L.; Luo, X.; Song, W.X.; Sharff, K.A.; Tang, N.; Haydon, R.C.; Luu, H.H.; He, T.C. Wnt signaling and human diseases: What are the therapeutic implications? *Lab. Invest.* **2007**, *87*, 97–103. [[CrossRef](#)]
47. Wang, H.; Charles, P.C.; Wu, Y.; Ren, R.; Pi, X.; Moser, M.; Barshishat-Kupper, M.; Rubin, J.S.; Perou, C.; Bautsch, V.; et al. Gene expression profile signatures indicate a role for Wnt signaling in endothelial commitment from embryonic stem cells. *Circ. Res.* **2006**, *98*, 1331–1339. [[CrossRef](#)]
48. Paling, N.R.; Wheadon, H.; Bone, H.K.; Welham, M.J. Regulation of embryonic stem cell self-renewal by phosphoinositide 3-kinase-dependent signaling. *J. Biol. Chem.* **2004**, *279*, 48063–48070. [[CrossRef](#)]
49. Cadigan, K.M.; Nusse, R. Wnt signaling: A common theme in animal development. *Genes Dev.* **1997**, *11*, 3286–3305. [[CrossRef](#)]
50. Glass, D.A.; Karsenty, G. In vivo analysis of Wnt signaling in bone. *Endocrinology.* **2007**, *148*, 2630–2634. [[CrossRef](#)]
51. Bergwitz, C.; Wendlandt, T.; Kispert, A.; Brabanta, G. Wnts differentially regulate colony growth and differentiation of chondrogenic rat calvaria cells. *Biochim. Biophys Acta.* **2001**, *1538*, 129–140. [[CrossRef](#)]
52. Fischer, L.; Boland, G.; Tuan, R.S. Wnt signaling during BMP-2 stimulation of mesenchymal chondrogenesis. *J. Cell Biochem.* **2002**, *84*, 816–831. [[CrossRef](#)] [[PubMed](#)]

53. Glass, D.A.; Karsenty, G. Molecular bases of the regulation of bone remodeling by the canonical Wnt signaling pathway. *Curr. Top. Dev. Biol.* **2006**, *73*, 43–84. [[CrossRef](#)] [[PubMed](#)]
54. Clevers, H. Wnt/beta-catenin signaling in development and disease. *Cell* **2006**, *127*, 469–480. [[CrossRef](#)]
55. He, T.C.; Sparks, A.B.; Rago, C.; Hermeking, H.; Zawel, L.; da Costa, L.T.; Morin, P.J.; Vogelstein, B.; Kinzler, K.W. Identification of c-MYC as a target of the APC pathway. *Science* **1998**, *281*, 1509–1512. [[CrossRef](#)]
56. Tetsu, O.; McCormick, F. Beta-catenin regulates expression of cyclin D1 in colon carcinoma cells. *Nature* **1999**, *398*, 422–426. [[CrossRef](#)]
57. He, T.C.; Chan, T.A.; Vogelstein, B.; Kinzler, K.W. PPAR delta is an APC-regulated target of nonsteroidal anti-inflammatory drugs. *Cell* **1999**, *99*, 335–345. [[CrossRef](#)]
58. Qu, Z.H.; Zhang, X.L.; Tang, T.T.; Dai, K.R. Promotion of osteogenesis through beta-catenin signaling by desferrioxamine. *Biochem. Biophys. Res. Commun.* **2008**, *370*, 332–337. [[CrossRef](#)]
59. Bain, G.; Muller, T.; Wang, X.; Papkoff, J. Activated beta-catenin induces osteoblast differentiation of C3H10T1/2 cells and participates in BMP2 mediated signal transduction. *Biochem. Biophys. Res. Commun.* **2003**, *301*, 84–91. [[CrossRef](#)]
60. Jackson, A.; Vayssiere, B.; Garcia, T.; Newell, W.; Baron, R.; Roman-Roman, S.; Rawadi, G. Gene array analysis of Wnt-regulated genes in C3H10T1/2 cells. *Bone*. **2005**, *36*, 585–598. [[CrossRef](#)]
61. Chang, J.; Sonoyama, W.; Wang, Z.; Jin, Q.; Zhang, C.; Krebsbach, P.H.; Giannobile, W.; Shi, S.; Wang, C.Y. Noncanonical Wnt-4 signaling enhances bone regeneration of mesenchymal stem cells in craniofacial defects through activation of p38 MAPK. *J. Biol. Chem.* **2007**, *282*, 30938–30948. [[CrossRef](#)] [[PubMed](#)]
62. Gaur, T.; Lengner, C.J.; Hovhannisyann, H.; Bhat, R.A.; Bodine, P.V.; Komm, B.S.; Javed, A.; van Wijnen, A.J.; Stein, J.L.; Stein, G.S.; et al. Canonical WNT signaling promotes osteogenesis by directly stimulating Runx2 gene expression. *J. Biol. Chem.* **2005**, *280*, 33132–33140. [[CrossRef](#)] [[PubMed](#)]
63. Day, T.F.; Guo, X.; Garrett-Beal, L.; Yang, Y. Wnt/beta-catenin signaling in mesenchymal progenitors controls osteoblast and chondrocyte differentiation during vertebrate skeletogenesis. *Dev. Cell* **2005**, *8*, 739–750. [[CrossRef](#)] [[PubMed](#)]
64. Dietrich, L.; Rathmer, B.; Ewan, K.; Bange, T.; Heinrichs, S.; Dale, T.C.; Schade, D.; Grossmann, T.N. Cell Permeable Stapled Peptide Inhibitor of Wnt Signaling that Targets β -Catenin Protein-Protein Interactions. *Cell Chem. Biol.* **2017**, *24*, 958–968. [[CrossRef](#)]
65. Ziegler, A. Thermodynamic studies and binding mechanisms of cell-penetrating peptides with lipids and glycosaminoglycans. *Adv. Drug Deliv. Rev.* **2008**, *60*, 580–594. [[CrossRef](#)]
66. Gallivan, J.P.; Dougherty, D.A. Cation- π interactions in structural biology. *Proc. Natl. Acad. Sci. USA.* **1999**, *96*, 9459–9464. [[CrossRef](#)]
67. Persson, S.; Killian, J.A.; Lindblom, G. Molecular ordering of interfacially localized tryptophan analogs in ester- and ether-lipid bilayers studied by 2H-NMR. *Biophys. J.* **1998**, *75*, 1365–1371. [[CrossRef](#)]
68. Qian, Z.; Martyna, A.; Hard, R.L.; Wang, J.; Appiah-Kubi, G.; Coss, C.; Phelps, M.A.; Rossmann, J.S.; Pei, D. Discovery and mechanism of highly efficient cyclic cell-penetrating peptides. *Biochemistry* **2016**, *55*, 2601–2612. [[CrossRef](#)]
69. Brock, R. The uptake of arginine-rich cell-penetrating peptides: putting the puzzle together. *Bioconjug. Chem.* **2014**, *25*, 863–868. [[CrossRef](#)]
70. MacDonald, B.T.; Tamai, K.; He, X. Wnt/beta-catenin signaling: Components, mechanisms and diseases. *Dev. Cell* **2009**, *17*, 9–26. [[CrossRef](#)]
71. Peterson-Nedry, W.; Erdeniz, N.; Kremer, S.; Yu, J.; Baig-Lewis, S.; Wehrli, M.; Baig-Lewis, S.; Wehrli, M. Unexpectedly robust assembly of the Axin destruction complex regulates Wnt/Wg signaling in Drosophila as revealed by analysis in vivo. *Dev. Biol.* **2008**, *320*, 226–241. [[CrossRef](#)] [[PubMed](#)]
72. Salins, P.; Shawesh, S.; He, Y.; Dibrov, A.; Kashour, T.; Arthur, G.; Amara, F. Lovastatin protects human neurons against Abeta-induced toxicity and causes activation of beta-catenin-TCF/LEF signaling. *Neurosci. Lett.* **2007**, *412*, 211–216. [[CrossRef](#)] [[PubMed](#)]
73. Sun, Y.C. Examination of effects of GSK3beta phosphorylation, beta-catenin phosphorylation and beta-catenin degradation on kinetics of Wnt signaling pathway using computational method. *Theor. Biol. Med. Model.* **2009**, *6*, 13. [[CrossRef](#)] [[PubMed](#)]
74. Provencher, S.W.; Glöckner, J. Estimation of globular protein secondary structure from circular dichroism. *Biochemistry* **1981**, *20*, 33–37. [[CrossRef](#)]

75. Moreno, A.; Mas-Oliva, J.; Soriano-García, M.; Salvador-Oliver, S.; Bolaños-García, V.M. Turbidity as a useful optical parameter to predict protein crystallization by dynamic light scattering. *J. Mol. Struct.* **2000**, *19*, 243–256. [[CrossRef](#)]
76. Lowry, O.H.; Roberts, N.R.; Wu, M.-L.; Hixon, W.S.; Crawford, E.J. The quantitative histochemistry of brain, II: enzyme measurements. *J. Biol Chem.* **1954**, *207*, 19–37.
77. Bradford, M.M. A rapid and sensitive method for the quantitation of microgram quantities of protein utilizing the principle of protein-dye binding. *Anal. Biochem.* **1976**, *72*, 248–254. [[CrossRef](#)]



© 2020 by the authors. Licensee MDPI, Basel, Switzerland. This article is an open access article distributed under the terms and conditions of the Creative Commons Attribution (CC BY) license (<http://creativecommons.org/licenses/by/4.0/>).